



SEMA3G is a Key IRGPI and Correlates with Immune Infiltrates in Head and Neck Squamous Carcinoma

Jintao Yu¹; Xia Sun¹; Yichen Zhao²; Chang Zheng²; Baosen Zhou^{2*}

¹Department of Otolaryngology, The First Hospital of China Medical University, Shenyang, Liaoning, China.

²Department of Epidemiology and Evidence-based Medicine, The First Hospital of China Medical University, Shenyang, Liaoning, China.

*Corresponding Author(s): Baosen Zhou

Department of Epidemiology and Evidence-based Medicine, The First Hospital of China Medical University, Shenyang, Liaoning, China.
 Tel: 024-961200; Email: bszhou@cmu.edu.cn

Abstract

Head and neck cancer is the seventh most common type of cancer worldwide, and the development of immunotherapy is conducive to the preservation of function and the improvement of prognosis. We intersected the immune gene database ImmPort and InnateDB databases and selected specific modules by WGCNA. We performed uni-/multi-variate Cox regression analyses to screen their prognostic roles in HNSCC patients from TCGA. GO and KEGG were used to define the functional enrichment of specific immune gene modules. Three prognostic immune genes were identified as prognostic genes, including DEFB1, PTX3 and SEMA3G. According to the median risk scores of patients, we divided HNSCC patients into low- and high-risk subgroups. In addition, the expression levels of many immune checkpoints positively correlated with the expression of prognostic genes but also indicated the immuno-microenvironment status of HNSCC. Finally, we validated the correlation of clinical baseline information of prognostic model genes by qRT-PCR and we found SEMA3G inhibited HNSCC cell growth and migration in TU212 and Fadu cells. In conclusion, we established a risk model based on immune-related genes showing excellent prognostic prediction ability and we discovered for the first time that SEMA3G plays an oncogenic role in HNSCC.

Received: Apr 11, 2023

Accepted: May 04, 2023

Published Online: May 11, 2023

Journal: Annals of Epidemiology and Public Health

Publisher: MedDocs Publishers LLC

Online edition: <http://meddocsonline.org/>

Copyright: © Zhou B (2023). This Article is distributed under the terms of Creative Commons Attribution 4.0 International License

Keywords: Immune; TCGA; Head and Neck Squamous Cell Carcinoma; Prognosis.

Introduction

Head and Neck Squamous Cell Carcinoma (HNSCC) is a common malignant tumor that originates from the mucous epithelium of the oral cavity, pharynx, and larynx. HNSCC is a heterogeneous disease, which owing to the anatomical complexity of the subsites, caused various risk factors and complex treatment methods [1]. With the rapid development of immunotherapy, Immune Checkpoint Inhibitors (ICI) were approved by FDA for

the patients with advanced head and neck cancer. When the patients obtained positive biomarkers, such as PD1 or PDL1, pembrolizumab would be treated as first-line therapy in clinical treatment [2-4]. However, there are still a huge number of patients with HNSCC who cannot benefit from immune checkpoint inhibitors therapy. Thus, it is necessary to explore a reliable immune-related biomarker to predict the survival risk of HNSCC and affect the sensitivity and effectiveness of immunotherapy.



Cite this article: Jintao Y, Xia S, Yichen Z, Chang Z, Baosen Z. SEMA3G Is A Key IRGPI And Correlates with Immune Infiltrates In Head and Neck Squamous Carcinoma. A Epidemiol Public Health. 2023; 6(1): 1108.

Immune-Related Genes (IRGs) have been reported to be closely associated with the occurrence and development of cancer, and partial IRGs could be a potential biomarker and affect the tumor immune microenvironment [5]. In recent years, the relationship between immune genes and cancer development has attracted increasing attention from many researchers. With the purpose of new concepts and algorithms, more and more studies have focused on the characterization of immune genes for various types of cancer, such as hepatocellular carcinoma [6], clear cell renal cell carcinoma [7], epithelial ovarian cancer [8], and so on. In the meanwhile, there was also explored a potential prognostic biomarker and a new immunotherapy target through pan-cancer analysis [9]. The distinct risk IRGs influence tumor immune microenvironment (TIME), immune cell infiltration, and immune invasion, which would further affect the prognosis of HNSCC. Head and neck cancer is an intrinsically immune-suppressing disease and fewer patients responded well to the ICIs, it has fostered research into the immune landscape HNSCC concerning outcome [10]. The key challenge was the selection of suitable patients and identifying effective treatment regimens. To find out better curative effects and explore more treatment methods, many researchers have reported that the expression of immune-related genes was different among immune cells and influenced HNSCC patient prognosis [11,12]. Just like cancer-associated fibroblasts cell (CAFs), a common stromal cell, it has been reported to play important roles in HNSCC progression and prognosis, such as participation in tumor cell proliferation, angiogenesis, and immunosuppression [13]. Besides, more effective and individualized treatments have been trying further explored combined with the comprehensive analysis of genomics, transcriptomics, and proteomics [14-17].

In this study, we systematically filtrated and evaluated the IRGs and TIME characteristics of HNSCC patients by WGCNA by transcriptome expression data. Predicted function mechanism of IRGs and identified several potential IRGs to further construct a risk model to evaluate the prognosis and tumor immune microenvironment of disease. Finally, we selected markers supported by previous literature for verification and performed the correlation analysis with immune checkpoint, which maybe provide a new reference to enhance the sensitivity and effectiveness of immunotherapy.

Results

Differentially expressed immune-related genes and functional enrichment pathways from the TCGA-HNSC

Compared with the immune-related genes (downloaded from ImmPort and InnateDB) and differentially expression genes in the TCGA-HNSC patients' cohorts, we took the intersection of the two databases to a total of 6196 immune-related genes (**Supplementary Table S1**) and 591 different expression genes by limma R package (**Supplementary Table S2**), including 142 down genes and 449 up genes (**Figure 1**). Next, we performed enrichment analysis by Gene Ontology (GO) and Kyoto Encyclopedia of Genes and Genomes (KEGG) analysis, to realize related functions of selected genes (**Supplementary Table S3 and Supplementary Table S4**). The mainly function enrichment pathway contained cytokine-cytokine receptor interaction, PI3K-Akt signaling pathway, Epstein-Barr virus infection, JAK-STAT signaling pathway and MAPK signaling pathway in **Figure 2**. In addition, the bar plot and bubble plot displayed the result of GO enrichment analysis (**Supplementary Figure S1**).

Weighted genes co-expression network analysis (WGCNA) construction and module detection

To further select the key immune-related genes, we performed WGCNA to search the most clinically relevant modules and the selected soft threshold was 5 with scaled free R^2 more than 0.9. In the constructed co-expression network, turquoise model is the top significant modules in the network, which has significant difference between tumor and normal ($P < 0.001$). In turquoise module, 105 genes are positive expression in normal and negative expression in tumor (**Figure 1**).

Confirmation of the IRGs prognosis signature

Univariate and multivariate Cox analysis were performed to determine the independent prognostic genes for OS among 105 candidate genes and the prognostic model for HNSCC samples calculated by the formula. $Risk\ score = Expression\ (IRGs) \times Coefficient\ (IRGs)$. Baseline data of clinical information integrity 528 HNSC patients from TCGA cohort was showed in Supplementary Table S5. First, univariate Cox analysis showed that 6 immune-related genes had the risk of affecting the prognosis of patients (**Table 1**) and multivariate Cox analysis revealed three genes (DEFB1, PTX3, and SEMA3G) significantly affecting the OS of patients with HNSCC ($P < 0.05$) in Supplementary Figure S2. The Kaplan Meier (KM) survival curves were showed in **Supplementary Figure S3**. Next, the result of univariate and multivariate Cox analysis was performed the signature on the signature genes to construct nomogram (**Figure 3A**). And then, time dependent ROC curves were applied to evaluate the predictive accuracy of nomogram and immune-related gene risk model (**Figure 3B, C**). Calibration curves in 3-year and 5-year were used to assess the consistency between predicted and actual survival outcome (**Figure 3D, E**).

Evaluation and verification of the IRGPI risk prediction model

According to the median of risk score, patients were divided into high- risk and low-risk groups. The expression of these six genes, survival status and the risk score distribution were presented in **Figure 4A-C**. As the risk score increased, the death risk of patients increased and the survival time decreased (**Figure 4B, C**). In addition, we found the risk model was associated with clinical staging, particularly stage T and N (**Figure 4D**). Univariate Cox analysis indicated that the risk of Immune Related Genes Prognosis Index (IRGPI) was remarkably associated with OS [hazard ratio (HR): 1.729, 95% CI: 1.358-2.200, $p < 0.001$; **Figure 4E**] and multivariate Cox analysis further showed that IRGPI risk model was a predictor of OS (HR: 1.751, 95% CI: 1.380-2.223, $p < 0.001$; **Figure 4F**). The risk score was the key one in all groups (**Table 2**). The conclusion was validated in the GEO dataset, which confirmed that the mortality risk in high-risk group of IRGPI risk model was higher than low-risk group in the GSE85446 and GSE65858 validation dataset ($p < 0.001$; **Supplementary Figure S4**).

Correlation of the IRGPI signature with TME and immune cell infiltration and ICB therapy-related molecule susceptibility

According to the ciphersort results, we found that the high and low risk groups were mainly distributed in a subset of immune cells, including B cells native, plasma cells, T cells CD8, T cells follicular helper, T cells regulatory (Tregs), Macrophages M0, Dendritic cells activated, Mast cells resting, Mast cells activated and Eosinophils. Otherwise, patient survival time are influenced by dendritic cells resting, Macrophages M0, Macrophages M2,

Mast cells resting, NK cells resting and T cells CD8 ($P < 0.05$). In addition, according to the result of single-sample GSEA (ssGSEA), that a method estimated the relative abundance of each type of immune cells and relative immune signature enrichment scores in HNSCC. We found the high-risk group was significantly associated with many immune cell infiltration and generally low expression compared with normal tissue, which is further proofed characteristics of immunosuppressive disease in head and neck cancer (Figure 5). Interestingly, in the result of ciber-sort and ssGSEA, we found that macrophages M2 ($p < 0.001$) were more significant than overall macrophages ($p < 0.041$). It may be that different subtypes of macrophages play an antagonistic role. Based on the results of immune infiltration, we were plotted the survival curve ($p < 0.05$; Supplementary Figure S5) and we found 9 kinds of immune cell has a significant influence in this IRGPI model. There are 26 results has a discrepancy expression in different group (Figures 6) and in high-risk group 4 of them have an obviously worse prognosis than low-risk group in Supplementary Figure S6 ($P < 0.001$). In the meanwhile, to investigate the latent ICB immunotherapy treatment effect of IRGPI risk score model in patients with HNSCC, we analyzed the correlation between the ICB therapy key targets and Hub genes signature (Figure 7A). In addition, we found most of Hub genes were markedly positive correlated to ICB therapy key targets (Figure 7B-J), and HAVCR2 had a strong correlation with DEFB1 ($R = -0.093$; $p = 0.037$), PTX3 ($R = 0.2$; $p = 5.4e-06$) and SEMA3G ($R = 0.32$; $p = 5.4e-13$).

Experimental Validation *in vitro* and *in vivo*

To further validate the signature we constructed, we analyzed the expressions of three immune-related prognosis genes in 33 HNSCC samples and matched normal controls from the clinical cancer cohort. As shown in Supplementary Figure 7, the expressions of SEMA3G ($P < 0.05$) and DEFB1 ($P < 0.05$) were significantly up-regulated in HNSCC tissues compared with adjacent HNSCC tissue, while PTX3 ($P < 0.05$) expressed the opposite, which were consistent with our previous analysis from TCGA database. We calculated the risk scores of 33 HNSCC patients according to the four immune-related prognosis genes signature we established before. All 33 HNSCC patients were divided into high- and low-risk subgroups with the median of risk score. Chi-square test analysis demonstrated that high risk scores were related with tumor location ($P = 0.035$), and clinical T stage ($P < 0.001$) (Table 3). However, there was no significant difference between risk score and other clinical stage characteristics, such as N stage and clinical stage. The reason may be due to the insufficient number of clinical samples, and we will expand the number of clinical sample for further study in the future.

In addition, we further performed experimental analysis of genes in prognostic signatures to validate their function in HNSCC cell growth and migration. Since SEMA3G have relatively high coefficient levels and were robust in the previously constructed models, the oncogenic role of SEMA3G was assessed in further experiments. The level of SEMA3G mRNA expression were significantly down-regulated in TU212 and Fadu cell as compared with control BEAS-2B cells (Figure 8A). To explore the function of SEMA3G in an HNSCC cell line, we overexpressed SEMA3G in TU212 and Fadu cells. The mRNA expression was significantly upregulated (Figure 8B). In addition, CCK8 showed SEMA3G transfection reduced the proliferative capacity of

TU212 and Fadu cells (Figure 8C). Furthermore, transwell migration showed that SEMA3G overexpression significantly reduced TU212 and Fadu cells migration and invasion (Figure 8D). Wound healing assays indicated that TU212 and Fadu cells migration steadily decreased following SEMA3G transfection *in vitro* (Figure 8E). These results suggest that immunosuppression affects disease progression of HNSCC malignancy. Anti-SEMA3G medication has been suggested as a potential HNSCC treatment strategy.

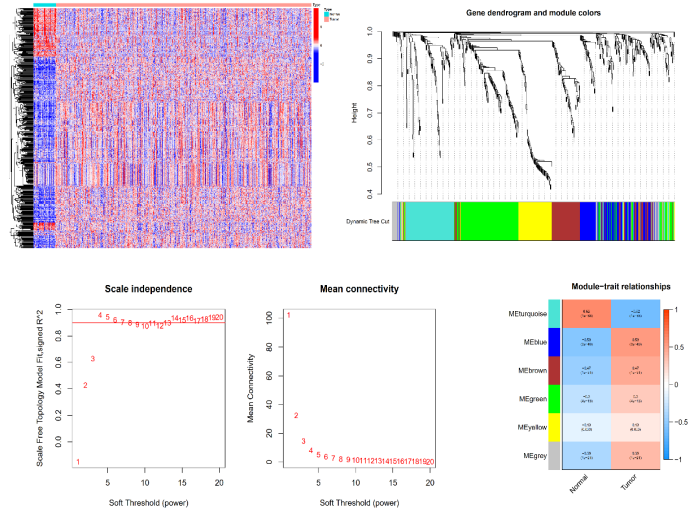


Figure 1: Identification and screening of immune-related HUB gene. (A) Heatmap plot for differentially expressed IRGs in TCGA-HNSCC. (B) Aberrant genes were displayed by cluster dendrogram and color of co-expression network modules from WGCNA. (C) Various soft-thresholding powers through scale-free fit index and mean connectivity. (D) The relationship between the modules and clinical traits in TCGA-HNSCC.

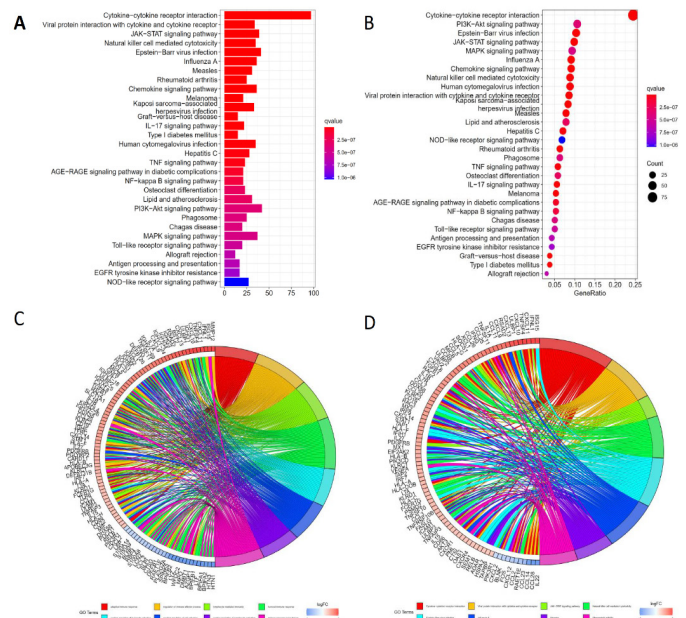


Figure 2: Gene ontology and KEGG analysis of the differentially expressed genes in TCGA-HNSCC. (A,B) KEGG enrichment analysis results for differential genes. (C) GO enrichment analysis results in circle plot. (D) KEGG enrichment analysis results in circle plot. KEGG, kyoto encyclopedia of genes and genomes.

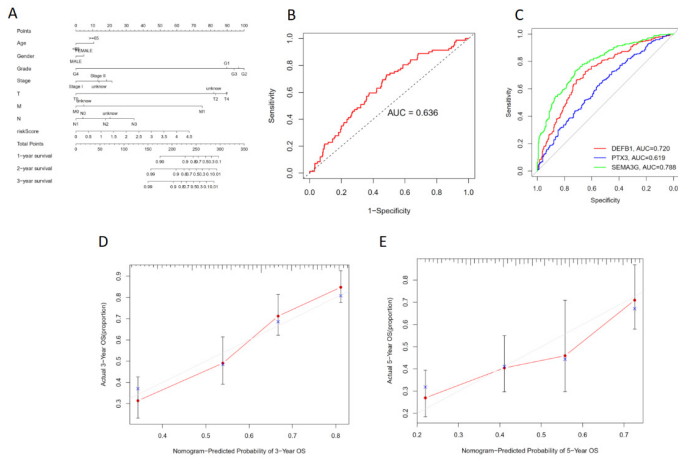


Figure 3: Confirmation of prognostic value of the IRPGs in HNSCC cases. **(A)** Nomogram was assembled by clinical characteristic and risk signature for predicting survival of HNSCC patients. **(B)** ROC analysis of the risk scores for overall prognosis prediction. The AUC was calculated for ROC curves, and sensitivity and specificity were calculated to assess score performance. Proportional hazards model results. **(C)** Areas under curves (AUCs) for predicting one year survival with DEFB1, PTX3 and SEMA3G. **(D,E)** 3-, 5- year nomogram calibration curves of entire TCGA cohort.

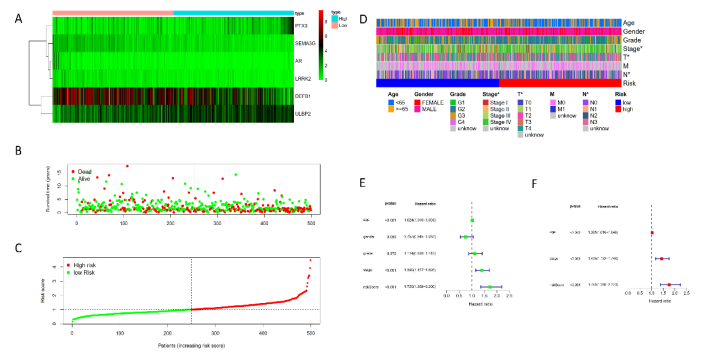


Figure 4: Confirmation of this immune-correlated mRNA risk model for forecasting HNSCC prognosis in the training set. **(A)** Heatmap of the 6 immune-related mRNA expression in HNSCC. The color from red to green shows a trend from high expression to low expression. **(B)** The survival status and duration of HNSCC patients. **(C)** Distribution of mRNA model risk score. **(D)** The heatmap plot of the IRGPI risk grouping and clinical characteristic. Age, Gender, Grade, Stage, T, M, N are shown as patient annotations. **(E, G)** Univariate and Multivariate Cox regression analysis results in the clinic pathologic factors and the risk score.

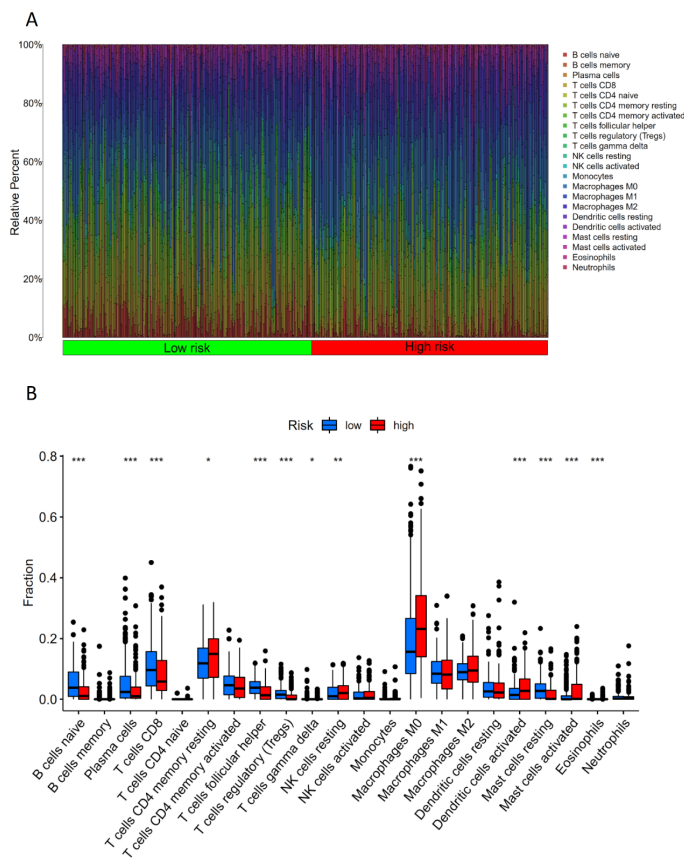


Figure 5: Tumor-infiltrating immune cells by different IRGPI group in head and neck carcinoma. **(A)** The landscape of 22 immune cells in each group. Each type of immune cell represented by various color. **(B)** The Wilcoxon rank-sum test displayed the difference in high and low IRGPs groups. (*, $P < 0.05$; **, $P < 0.01$; ***, $P < 0.001$).

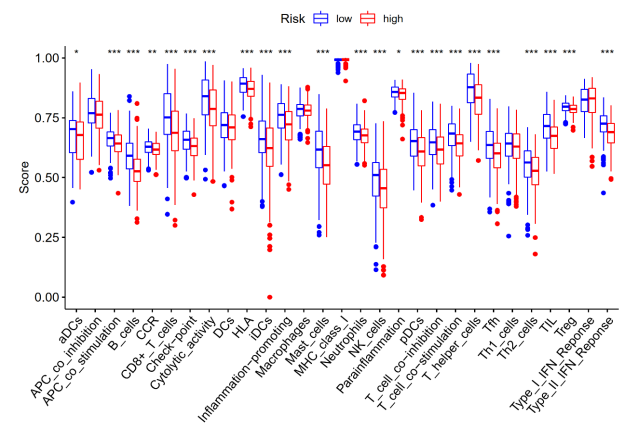


Figure 6: The function of tumor-infiltrating immune cells calculated by ssGSEA from different IRGPI group. (*, $P < 0.05$; **, $P < 0.01$; ***, $P < 0.001$).

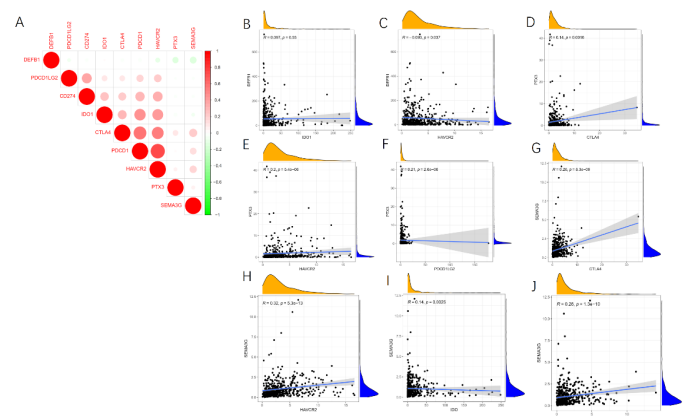


Figure 7: Correlation between immune check-point inhibitors and this IRGPI signature. **(A)** Correlation analyses between immune check-point inhibitors CD274, PDCD1, PDCD1LG2, CTLA4, HAVCR2, and IDO1 and our IRGPI signature. Correlation between this signature and CD8+T cells. **(B-J)** association between this signature and ICIs. $P < 0.05$.

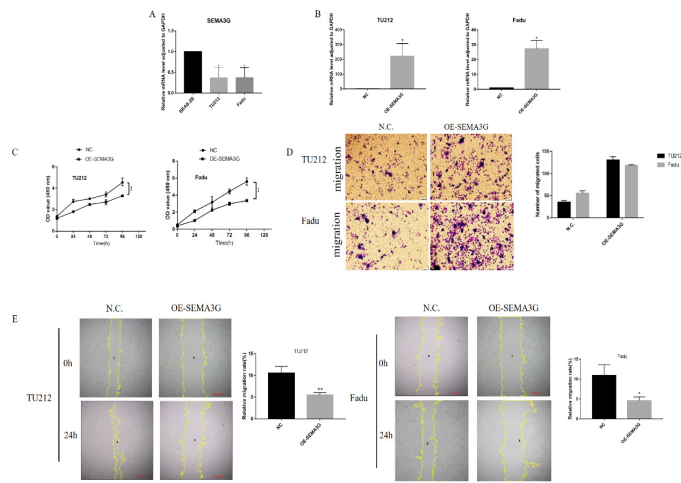


Figure 8: SEMA3G overexpression inhibits HNSCC cell line multiplication and migration capacity. SEMA3G (A) mRNA expression in HNSCC cell lines and normal human respiratory tract epithelial cells. SEMA3G (B) mRNA expression in TU212 and Fadu cell lines transfected with overexpression SEMA3G plasmid. (C) Proliferation assays were performed in TU212 and Fadu cells through CCK-8 assay when SEMA3G was overexpressed. (D) Transwell migration assay of TU212 and Fadu cell lines treated with SEMA3G overexpression. (E) Wound healing assays of TU212 and Fadu cell lines treated with SEMA3G overexpression. *P < 0.05.

Table 1: Univariate Cox analysis showed 6 IRGs affecting the HNSCC prognosis.

| id | HR (95% CI) | P value |
|--------|-----------------|---------|
| AR | 0.68(0.48-0.97) | 0.034 |
| DEFB1 | 1.00(1.00-1.00) | 0.036 |
| LRRK2 | 0.69(0.49-0.96) | 0.030 |
| PTX3 | 1.03(1.00-1.05) | 0.036 |
| SEMA3G | 0.78(0.65-0.94) | 0.009 |
| ULBP2 | 1.02(1.00-1.03) | 0.030 |

CI: confidence interval; HR: Hazard ratio.

Table 2: Univariate and multivariate Cox regression analysis.

| Variable | Univariate Cox regression | | Multivariate Cox regression | |
|------------|---------------------------|---------|-----------------------------|---------|
| | HR(95% CI) | P value | HR(95% CI) | P value |
| Age | 1.03(1.01-1.04) | <0.001 | 1.31(1.02-1.05) | <0.001 |
| Gender | 0.76(0.55-1.05) | 0.098 | | |
| Grade | 1.11(0.88-1.41) | 0.375 | | |
| Stage | 1.40(1.16-1.69) | <0.001 | 1.44(1.18-1.75) | <0.001 |
| Risk Score | 1.73(1.36-2.20) | <0.001 | 1.75(1.38-2.22) | <0.001 |

CI: confidence interval; HR: Hazard ratio.

Discussion

Given the complexity anatomical structure and daily functions in the head and neck area, HNSCC patients would face disabilities, so such as losing working ability, which can also affect families [18]. Thus, we are committed to exploring new treatment options, to increase the choice of treatment methods and construct a prognosis model for HNSCC patients. In recent year, there have been substantial significant research on the screening of IRGPI and clinical drug based on TCGA mRNA sequence, but the accuracy of survival estimation and the number of pa-

Table 3: Associations between risk scores and clinicopathological characteristics in clinical HNSCC cohort.

| Characteristics | Total | Risk Scores | | P value |
|------------------------|-------|-----------------|------------------|---------|
| | | Low (n=17) 2.68 | High (n=16) 2.68 | |
| Age,ys | 33 | | | |
| ≤60 | 16 | 9 | 8 | 0.500 |
| >60 | 18 | 8 | 8 | |
| Gender | | | | 0.700 |
| Male | 30 | 16 | 14 | |
| Female | 4 | 2 | 2 | |
| Smoking | | | | 0.093 |
| Yes | 25 | 15 | 10 | |
| None | 9 | 2 | 6 | |
| Drinking | | | | 0.270 |
| Yes | 22 | 10 | 12 | |
| None | 12 | 7 | 4 | |
| Location | | | | 0.035 |
| Larynx | 12 | 8 | 4 | |
| Hypopharynx | 9 | 2 | 5 | |
| Oral cavity+oropharynx | 12 | 7 | 7 | |
| T stage | | | | <0.001 |
| I+II+III | 19 | 16 | 2 | |
| IV | 15 | 1 | 14 | |
| N stage | | | | 0.410 |
| 0 | 12 | 7 | 5 | |
| I+II+III | 22 | 10 | 11 | |
| Clinical stage | | | | 0.071 |
| I+II+III | 9 | 7 | 2 | |
| IV | 25 | 10 | 14 | |

TNM stage, clinical tumor-node-metastasis stage; *P <0.05 was considered statistically significant; Values are mean ± standard deviation or n (%)

tients who benefit were still limited [19-22]. In this study, we developed an IRGPI model based on TCGA-HNSCC and validated by the GEO database and histological experiment. We further explored the immune cell distribution and immune cell infiltration and further stratified clinically defined groups of patients (e.g., clinical stage and pathological grade) into subgroups with different survival outcomes. In this research, we explored potential molecular biomarkers related to treatment efficacy to provide a newly prognostic biomarker for HNSCC patients.

As we all know, many researchers focused on tumor immunity, believing that it promoted the tumor immune microenvironment and the development of immunotherapy, which means we harvested a deeper understanding of HNSCC development and treatment. But, unfortunately, the impact of an effective complete immunotherapy database on the survival outcome of HNSCC patients is lacking, which needs more researchers to collect and dispose of data. *Jingrun Yanga*, used cluster, and PCA analysis, and identified six immunity gene signatures for predicting the prognosis of HNSCC [5]. *Yue Chen1*, reported that they developed a prognostic marker to predict the prognosis of both conventional therapy and immunotherapy [19]. *Hyun Chang*, CD200R1, a variety of immune mechanisms, is related

to an immune-rich microenvironment with high immune cell estimates [12]. No matter how mutated the germline genetic information is, it would reshape the tumor microenvironment functional mechanisms and modulatory genes process [23]. Ultimately, achievements in scientific research could lead to the development of personalized therapeutic strategies. In this research, we identified 3 key Immune-related prognostic genes from 525 HNSCC patients. Three of seven IRGPI were reported to be involved in tumorigenesis and progression, but there have been few regarded reports and lacking tissue and cytological experiments. The higher level of DEFB1 targeted inhibition of PI3K/mTOR signaling pathway to effectively antitumor [24]. SEMA3G also takes part in tumors of the reproductive system and nervous system [25,26]. The higher expression of PTX3 would promote esophageal squamous cell carcinoma occurrence and promote cancer migration by a toll-like receptor 4 (TLR4)/NF-kappaB signaling pathway [27,28]. The difference in disease prognosis and tumor clinical stage showed the various situation of PTX3 expression [27,29]. Research suggested that PTX3 affects the prognosis of a tumor by regulating stem cell and macrophage polarization [30]. Other studies have shown that PTX3 can promote epidermal growth factor secretion to enhance head and neck cellular biological behavior [31,32]. Therefore, we hope our results would help to identify the IRGPI risk model for HNSCC, providing insights into the development of novel biomarkers and further research into individualized targeted drug therapy.

In this research, according to the result of ciphersort and ssGSEA, we found the different expressions of risk genes influence immune cell distribution and immune cell infiltration, which can be exploited to promote tumor cells metastasis, angiogenesis, and growth. Interesting, we definitely find differences between multiple immune cells in the high - and low-risk groups and different subtypes of immune cells play different roles in our results, such as M1 macrophages and M2 macrophages. Besides, these also affected the survival of HNSCC patients, which made exploring the effectiveness of the response to immunotherapy meaningful. The immune system can produce immunosuppressive mediators and promote immunomodulatory cell types to evade the host immune in HNSCC [33]. In head and neck cancer, different anatomical subsite and etiological agent will be infiltrated variously by the extent and composition of the immune cell [34]. A recent study suggested stromal components played an important role in the development, establishment, and progression of HNSCC [35]. The tumor microenvironment consisted of tumor cells and stromal cells, which include endothelial cells, cancer-associated fibroblasts (CAFs), and immune cells [35]. Each ingredient performs a variety of functions to influence the occurrence and development of tumors. For example, Cancer-Associated Fibroblasts (CAFs) can stimulate phenotypic transformation and secrete a broad range of growth factors [36]. In addition, in a recent study, pirfenidone was regarded as a potential drug for suppressing invasion and potential metastasis in breast cancer [13]. Tumor-Associated Macrophages (TAMs) also could be induced M2-polarization by cytokines released by tumor cells [37]. Thus, the prognosis of tumor patients may not only be due to the changes expression of genes in tumor cells but also tumor microenvironment especially the stromal composition of the HNSCC, which maybe provide a new clinical intervention.

We tried to include more databases to rigorously validate our biomarkers, but survival data sets and ICI therapy effectiveness in HNSCC were not so much available. In addition, accord-

ing to the etiology and site of disease leading to heterogeneity in tumor prognosis, multiple omics studies may be more conducive to assessing the risk and prognosis of HNSCC [38]. More functional experiments in the laboratory and more clinical trials needs to verify this risk model. And the interaction analysis with the characteristic risk factors of HNSCC need further verification in the future, such as smoking, HPV infection, and TP53 high expression.

In conclusion, our study proved that these six IRGPI risk score models were significantly correlated with HNSCC prognosis and immune infiltration. In addition, we built a prognostic model to evaluate the correlation of ICIs genes in HNSCC. These results provide novel biomarkers and promising avenues for immunotherapy in HNSCC.

Materials and methods

Data download

546 HNSCC samples RNA sequencing [fragments per kilo base of transcript per million mapped reads (FPKM) values] data and their clinical information were downloaded from The Cancer Genome Atlas (TCGA) database (<https://portal.gdc.cancer.gov/projects/TCGA-HNSC>), including 502 cancer samples and 44 normal samples. 270 HNSCC samples (GSE65858) and 66 HNSCC samples (GSE85446) RNA sequencing and the survival information were downloaded from the Gene Expression Omnibus (GEO) database (<https://www.ncbi.nlm.nih.gov/geo/>). The lists of immune-related genes were downloaded from the ImmPort (<https://www.immport.org/shared/home>) and InnateDB (<https://www.innatedb.com/>) databases.

Identification immune-related hub genes and function of enrichment analysis

Based on RNA-sequence data of HNSCC samples (502 tumors vs. 44 normal samples) obtained from TCGA database, the lists of differentially expressed genes ($FDR < 0.05$, $|\logFC| > 1$) were identified by using the limma package of R [39]. After intersection the context of the immune-related gene lists obtained from ImmPort and InnateDB. The key selected differentially expressed genes were obtained and further analyzed by using Gene Ontology (GO) and Kyoto Encyclopedia of Genes and Genomes (KEGG) analyses with the clusterProfiler package of R [40].

WGCNA

Weighted Gene Co-expression Network Analysis (WGCNA) is a method capable of exploring the relationship of clusters (modules) of highly correlated genes and external sample traits [41]. In our study, whole immune-related genes DEGs (according to P) were constructed by using the expression data of TCGA cohort by calculating the Pearson correlation coefficient. The similarity matrix was transformed into an adjacency matrix with a network type of signed and a soft threshold of 5 and then transformed into a topological matrix with the Topological Overlap Measure (TOM) describing the degree of association between genes. 1-TOM was used as the distance to cluster the genes, and then the dynamic pruning tree was built to identify the modules. Finally, we identified seven modules by setting the merging threshold function at 0.3. The highest correlation modules (turquoise modules) with clinical traits were regarded as key module and selected to identify as significantly tumor-associated immune-related hub genes for further analysis.

Generation of the Risk Score

The prognostic analysis was performed for each gene (total 115) in the turquoise modules using a univariate Cox regression model. A total of 7 genes with significant prognosis and clinical traits were extracted for further multivariate Cox regression analysis. To validate the prognostic value of this model, we evaluated IRGS by Kaplan Meier (KM) survival curves with log-rank tests and built a nomogram to predict survival probabilities of HNSCC at 3, 5 years. Then, we compared baseline information with two IRGs subgroups, which divide the samples with high (n=251) and low (n=251) risk groups using the limma package of R, and the results are presented in a landscape map.

Tumor immune microenvironment and Immune checkpoint blockade

In TCGA 502 HNSCC samples expression data was imported into CIBERSORT (<https://cibersort.stanford.edu/>) to estimate the relative proportion of 22 types of immune cells. Then single sample GSEA (ssGSEA) analysis was performed on several representative gene sets with the GSVA package of R, and KM survival curves were used to explore the survival of different immune cells types in different risk subtypes [42]. To further explore enhanced immunotherapy effectiveness, we evaluated the relationship among hub genes and six key genes of immune checkpoint inhibitors therapy, including programmed death 1 (PDCD1), programmed death ligand 1 (CD274), programmed death ligand 2 (PDCD1LG2), T-cell immunoglobulin domain and mucin domain-containing molecule-3 (HAVCR2), cytotoxic T-lymphocyte antigen 4 (CTLA-4), and indoleamine 2, 3- dioxygenase 1 (IDO1) in HNSCC [43]. We analyzed the interaction and correlation between selected immune-related prognosis genes and these six immune checkpoint blockade key genes expression.

Patients and samples

We collected 34 patients with squamous cell carcinoma of the head and neck from the Department of Otolaryngology of the First Affiliated Hospital of China Medical University and were diagnosed with squamous cell carcinoma of the head and neck by the pathologist. All patients included in the study signed an informed consent form, and the whole consent procedure was approved by the ethical standards defined by Institutional Ethics Review Committee of The First Affiliated Hospital of China Medical University (Approval number 2022-24-2). We respectively defined the central part of the tumor and the part 1cm away from the cancer as cancer and normal tissue. The clinical information of patients is summarized in **Table 3**.

Cell Culture and Transfection

Thanks to the Department of Genetics, China Medical University granted the Head and neck cancer cell lines (TU212 and Fadu) and human respiratory epithelium cell line (BEAS-2B). BEAS-2B cells were cultivated in DMEM and TU212 cells were cultivated in 1640 with 10% fetal bovine serum (FBS), along with 100 U/mL penicillin and streptomycin and Fadu cells were cultivated in MEM with 10% fetal bovine serum (FBS), along with 100 U/mL penicillin and streptomycin. The expression vectors for SEMA3G were designed and synthesized (Syngentbio). Over expression and control vectors were transfected into TU212 and Fadu cells using the lipofectamine 8000 protocol (beyotime) [44].

qRT-PCR

Total RNA was extracted from the patient's tumor and normal tissues using TRIZOL reagent (Vazyme, Nanjing, China) and reverse-transcribed to cDNA using HiScript[®] III RT SuperMix for qPCR (+gDNA wiper) (Vazyme, Nanjing, China), following the manufacturer's instructions. Then, qRT-PCR was performed using ChamQ SYBR qPCR Master Mix (Without ROX) (Vazyme, Nanjing, China). The expression levels were normalized to the internal control, glyceraldehyde-3-phosphate dehydrogenase (GAPDH), and relative expressions were calculated by the 2^{-ΔΔCt} method. Primer designs were derived from PRIMER bank (<https://pga.mgh.harvard.edu/primerbank/>) and Primer synthesis were derived from GENEWIZ. The primer sequences were as follows:

PTX3 Forward primer (5'-3'): CATCTCCTTGCGATTCTGTTTGG;

PTX3 Reverse Primer (5'-3'): CCATTCCGAGTGCTCCTGA;

SEMA3G Forward primer (5'-3'): CAGAGGATGGGACCTACGATG;

SEMA3GC Reverse Primer (5'-3'): GTTGGCACCTTAAACACCTGG;

DEFB1 Forward primer (5'-3'): ATGAGAACTTCCTACCTTCTGCT;

DEFB1 Reverse Primer (5'-3'): TCTGTAAACAGGTGCCTGAATTT;

GAPDH Forward primer (5'-3'): GGAGCGAGATCCCTCCAAAAT;

GAPDH Reverse Primer (5'-3'): GGCTGTTGTCATACTTCTCATGG;

Cell Counting Kit-8 (CCK-8)

The control group and cells with high SEMA3G expression were digested with trypsin, and complete medium was used to suspend the cells, adjusting the density to 2000 cells/well. The cells were inoculated in a 96-well plate and put the plate in the incubator for the appropriate time (e.g., 6, 12, 24, or 48 hours). Add 10 μL of CCK8 solution to each well of the plate using a repetitive pipette and put plates in the incubator for 2 hours, and using an enzyme marker measured absorbance at 450 nm and Image J software.

Transwell Assay

To explore the function of SEMA3G in an HNSCC cell line, over expression and control vectors were transfected into TU212 and Fadu cells using the lipofectamine 3000 protocol. 24 hours after transfection, the transformed cells (5x10⁴) were suspended in 200 μL serum-free medium and inoculated into the upper chamber. 600 μL complete medium containing 10% was added to the lower chamber. The transwell device was then incubated for 2 days, cells in the inferior chamber were fixed with 4% formaldehyde for 15 min, and dyed with 0.1% crystal violet for 15 min. Cells in the upper chamber were removed with a cotton swab. Cell migration was observed using an inverted microscope (Olympus, Japan).

Wound Healing Assay

Draw a horizontal line on the bottom of a 6-well plate covered with cells. Next day, 100μL tip head used to make a scratch on the bottom and intersected with the mark line. And then, the cells were washed 2–3 times with PBS and fresh serum-free medium was added. The cells were incubated for 24 hours, observed under a microscope and photographed. The proportion of migrated cells was calculated using Image J software.

Statistical analysis

An independent t test was performed to compare continuous variables between two groups. Univariate survival analysis was performed by K-M survival analysis with the log-rank test. Multivariate survival analysis was performed using the Cox regression model. Associations between risk scores and other clinical features in HNSCC patients were analyzed with Fisher exact test or chi-square test. A two-sided $P < 0.05$ was considered significant.

Acknowledgements

Thanks to all the authors who participated in this study.

Author contributions

B.Z contributed to the study design. Y.Z and C.Z were responsible for data acquisition, bioinformatics analysis, and data visualization; J.Y drafted the original manuscript. X.S read and revised the original manuscript. All authors have approved the publication of this study.

Funding

This research received no funding.

Data availability statement

All data supporting the findings of this study are available within the article and its Supplementary Materials. Our study was mainly based on open access TCGA and GEO databases, which can be downloaded relevant data for research and publish relevant articles. All methods were carried out in accordance with relevant guidelines and regulations.

Ethics declarations

All experimental protocols were approved by Institutional Ethics Review Committee of The First Affiliated Hospital of China Medical University (approval number 2022-24-2). Informed consent was obtained from all subjects involved in the study.

Additional Information

The authors declare that they have no competing interests.

References

- Johnson DE, Burtneß B, Leemans CR, Lui VWY, Bauman JE, et al. Head and neck squamous cell carcinoma. *Nat Rev Dis Primers*. 2020; 6: 92.
- Cramer JD, Burtneß B, Le QT Ferris RL. The changing therapeutic landscape of head and neck cancer. *Nat Rev Clin Oncol*. 2019; 16: 669-683.
- Thorsson V, Gibbs DL, Brown SD, Wolf D, Bortone DS, et al. The Immune Landscape of Cancer. *Immunity*. 2018; 48: 812-30 e14.
- Ferris RL. Immunology and Immunotherapy of Head and Neck Cancer. *J Clin Oncol*. 2015; 33: 3293-304.
- Yang J, Xie K Li C. Immune-related genes have prognostic significance in head and neck squamous cell carcinoma. *Life Sci*. 2020; 256: 7906.
- Gong J, Li R, Chen Y, Zhuo Z, Chen S, et al. HCC subtypes based on the activity changes of immunologic and hallmark gene sets in tumor and nontumor tissues. *Brief Bioinform*. 2021; 22.
- Yin X, Wang Z, Wang J, Xu Y, Kong W, et al. Development of a novel gene signature to predict prognosis and response to PD-1 blockade in clear cell renal cell carcinoma. *Oncoimmunology*. 2021; 10: 1933332.
- Li H, Wu M, Wu Z, Liang J, Wang L, et al. Prognostic value of preoperative soluble interleukin 2 receptor alpha as a novel immune biomarker in epithelial ovarian cancer. *Cancer Immunol Immunother*. 2021; 71: 1519-1530.
- Jiang ZH, Shen X, Wei Y, Chen Y, Chai H, et al. A Pan-Cancer Analysis Reveals the Prognostic and Immunotherapeutic Value of Stanniocalcin-2 (STC2). *Front Genet*. 2022; 13: 927046.
- Leemans CR, Snijders PJF, Brakenhoff RH. The molecular landscape of head and neck cancer. *Nat Rev Cancer*. 2018; 18: 269-282.
- Tao W, Tian G, Xu S, Li J, Zhang Z, Li J. NAT10 as a potential prognostic biomarker and therapeutic target for HNSCC. *Cancer Cell Int*. 2021; 21: 413.
- Chang H, Lee YG, Ko YH, Cho JH, Choi JK, et al. Prognostic Value of CD200R1 mRNA Expression in Head and Neck Squamous Cell Carcinoma. *Cancers (Basel)*. 2020; 12: 13.
- Es HA, Cox TR, Sarafraz-Yazdi E, Thiery JP, Warkiani ME. Pirfenidone Reduces Epithelial-Mesenchymal Transition and Spheroid Formation in Breast Carcinoma through Targeting Cancer-Associated Fibroblasts (CAFs). *Cancers (Basel)*. 2021;13: 5118.
- Stenzinger A, Endris V, Budczies J, Merkelbach-Bruse S, Kazdal D, et al. Harmonization and Standardization of Panel-Based Tumor Mutational Burden Measurement: Real-World Results and Recommendations of the Quality in Pathology Study. *J Thorac Oncol*. 2020; 15: 1177-1189.
- Sun R, Limkin EJ, Vakalopoulou M, Dercle L, Champiat S, et al. A radiomics approach to assess tumour-infiltrating CD8 cells and response to anti-PD-1 or anti-PD-L1 immunotherapy: an imaging biomarker, retrospective multicohort study. *The Lancet Oncology*. 2018; 19: 1180-1191.
- Long Q, Huang C, Meng Q, Peng J, Yao F, et al. TNF Patterns and Tumor Microenvironment Characterization in Head and Neck Squamous Cell Carcinoma. *Front Immunol*. 2021; 12: 754818.
- Yin L, Zhou L, Xu R. Identification of Tumor Mutation Burden and Immune Infiltrates in Hepatocellular Carcinoma Based on Multi-Omics Analysis. *Front Mol Biosci*. 2020; 7: 599142.
- Bonomo P, Paderno A, Mattavelli D, Zenda S, Cavaliere S, Bossi P. Quality Assessment in Supportive Care in Head and Neck Cancer. *Front Oncol*. 2019; 9: 926.
- Chen Y, Li ZY, Zhou GQ, Sun Y. An Immune-Related Gene Prognostic Index for Head and Neck Squamous Cell Carcinoma. *Clin Cancer Res*. 2021; 27: 330-341.
- Li B, Cui Y, Diehn M, Li R. Development and Validation of an Individualized Immune Prognostic Signature in Early-Stage Non-squamous Non-Small Cell Lung Cancer. *JAMA Oncol*. 2017; 3: 1529-1537.
- Yang J-L, Wang CCN, Cai J-H, Chou C-Y, Lin Y-CHung C-C. Identification of GSN and LAMC2 as Key Prognostic Genes of Bladder Cancer by Integrated Bioinformatics Analysis. *Cancers*. 2020; 12: 7.
- Dai Y, Qiang W, Lin K, Gui Y, Lan X, Wang D. An immune-related gene signature for predicting survival and immunotherapy efficacy in hepatocellular carcinoma. *Cancer Immunol Immunother*. 2021; 70: 967-979.
- Sayaman RW, Saad M, Thorsson V, Hu D, Hendrickx W, et al. Germline genetic contribution to the immune landscape of cancer. *Immunity*. 2021; 54: 367-86.e8.

24. Lee M, Wiedemann T, Gross C, Leinhäuser I, Roncaroli F, et al. Targeting PI3K/mTOR Signaling Displays Potent Antitumor Efficacy against Nonfunctioning Pituitary Adenomas. *Clin Cancer Res.* 2015; 21: 3204-3215.
25. Oleari R, Andre V, Lettieri A, Tahir S, Roth L, et al. A Novel SEMA3G Mutation in Two Siblings Affected by Syndromic GnRH Deficiency. *Neuroendocrinology.* 2021; 111: 421-41.
26. Ji C, Wang Y, Wang Y, Luan J, Yao L, et al. Immune-related genes play an important role in the prognosis of patients with testicular germ cell tumor. *Ann Transl Med.* 2020; 8: 866.
27. Rathore M, Girard C, Ohanna M, Tichet M, Jouira RB, et al. Cancer cell-derived long pentraxin 3 (PTX3) promotes melanoma migration through a toll-like receptor 4 (TLR4)/NF-kappaB signaling pathway. *Oncogene.* 2019; 38: 5873-5889.
28. Fan Z, Zheng Y, Li X, Deng X, Ba Y, et al. Promoting role of pentraxin-3 in esophageal squamous cell carcinoma. *Mol Ther Oncolytics.* 2022; 24: 772-787.
29. Falagarío UG, Busetto GM, Netti GS, Sanguedolce F, Selvaggio O, et al. Prospective Validation of Pentraxin-3 as a Novel Serum Biomarker to Predict the Risk of Prostate Cancer in Patients Scheduled for Prostate Biopsy. *Cancers (Basel).* 2021; 13: 7.
30. Cui X, Qin T, Zhao Z, Yang G, Pires Sanches JG, et al. Pentraxin-3 inhibits milky spots metastasis of gastric cancer by inhibiting M2 macrophage polarization. *J Cancer.* 2021; 12: 4686-4897.
31. Chan SH, Tsai JP, Shen CJ, Liao YH, Chen BK. Oleate-induced PTX3 promotes head and neck squamous cell carcinoma metastasis through the up-regulation of vimentin. *Oncotarget.* 2017; 8: 41364-41378.
32. Chang WC, Wu SL, Huang WC, Hsu JY, Chan SH, et al. PTX3 gene activation in EGF-induced head and neck cancer cell metastasis. *Oncotarget.* 2015; 6: 7741-7757.
33. Wang C, Li Y, Jia L, Kim JK, Li J, et al. CD276 expression enables squamous cell carcinoma stem cells to evade immune surveillance. *Cell Stem Cell.* 2021; 28: 1597-1613 e7.
34. Mody MD, Rocco JW, Yom SS, Haddad RISaba NF Head and neck cancer. *Lancet.* 2021; 398: 2289-2299.
35. Peltanova B, Raudenska M, Masarik M. Effect of tumor microenvironment on pathogenesis of the head and neck squamous cell carcinoma: a systematic review. *Mol Cancer.* 2019; 18: 63.
36. Canning M, Guo G, Yu M, Myint C, Groves MW, et al. Heterogeneity of the Head and Neck Squamous Cell Carcinoma Immune Landscape and Its Impact on Immunotherapy. *Front Cell Dev Biol.* 2019; 7: 52.
37. Zhou WH, Wang Y, Yan C, Du WD, Al-Aroomi MA, et al. CC chemokine receptor 7 promotes macrophage recruitment and induces M2-polarization through CC chemokine ligand 19&21 in oral squamous cell carcinoma. *Discov Oncol.* 2022; 13: 67.
38. Giacomini A, Ghedini GC, Presta M, Ronca R. Long pentraxin 3: A novel multifaceted player in cancer. *Biochim Biophys Acta Rev Cancer.* 2018; 1869: 53-63.
39. Ritchie ME, Phipson B, Wu D, Hu Y, Law CW, et al. limma powers differential expression analyses for RNA-sequencing and microarray studies. *Nucleic Acids Res.* 2015; 43: e47.
40. Yu G, Wang LG, Han YHe QY. Cluster Profiler: an R package for comparing biological themes among gene clusters. *OMICS.* 2012; 16: 284-287.
41. Ghazalpour A, Doss S, Zhang B, Wang S, Plaisier C, et al. Integrating genetic and network analysis to characterize genes related to mouse weight. *PLoS Genet.* 2006; 2: e130.
42. Hanzelmann S, Castelo RGuinney J. GSVA: gene set variation analysis for microarray and RNA-seq data. *BMC Bioinformatics.* 2013; 14: 7.
43. Xu Q, Wang YHuang W. Identification of immune-related lncRNA signature for predicting immune checkpoint blockade and prognosis in hepatocellular carcinoma. *Int Immunopharmacol.* 2021; 92: 107333.
44. Singharajkomron N, Yodsurang V, Seephan S, Kungsukool S, Petchjorm S, et al. Evaluating the Expression and Prognostic Value of Genes Encoding Microtubule-Associated Proteins in Lung Cancer. *Int J Mol Sci.* 2022; 23: 23.